View metadata, citation and similar papers at core.ac.uk
brought to you by CORE
provided by Lancaster E-Prints

Event Excess in the MiniBooNE Search for $\bar{\nu}_\mu \to \bar{\nu}_e$ Oscillations

A. A. Aguilar-Arevalo,[12] C. E. Anderson,[15] S. J. Brice,[6] B. C. Brown,[6] L. Bugel,[11] J. M. Conrad,[11] R. Dharmapalan,[1] Z. Djurcic,[2] B. T. Fleming,[15] R. Ford,[6] F. G. Garcia,[6] G. T. Garvey,[9] J. Mirabal,[9] J. Grange,[7] J. A. Green,[8,9] R. Imlay,[10] R. A. Johnson,[3] G. Karagiorgi,[11] T. Katori,[8,11] T. Kobilarcik,[6] S. K. Linden,[15] W. C. Louis,[9] K. B. M. Mahn,[5] W. Marsh,[6] C. Mauger,[9] W. Metcalf,[10] G. B. Mills,[9] C. D. Moore,[6] J. Mousseau,[7] R. H. Nelson,[4] V. Nguyen,[11] P. Nienaber,[14] J. A. Nowak,[10] B. Osmanov,[7] Z. Pavlovic,[9] D. Perevalov,[1] C. C. Polly,[6] H. Ray,[7] B. P. Roe,[13] A. D. Russell,[6] R. Schirato,[9] M. H. Shaevitz,[5] M. Sorel,[5,*] J. Spitz,[15] I. Stancu,[1] R. J. Stefanski,[6] R. Tayloe,[8] M. Tzanov,[4] R. G. Van de Water,[9] M. O. Wascko,[10,†] D. H. White,[9] M. J. Wilking,[4] G. P. Zeller,[6] and E. D. Zimmerman[4]

(MiniBooNE Collaboration)

[1]*University of Alabama, Tuscaloosa, Alabama 35487, USA*
[2]*Argonne National Laboratory, Argonne, Illinois 60439, USA*
[3]*University of Cincinnati, Cincinnati, Ohio 45221, USA*
[4]*University of Colorado, Boulder, Colorado 80309, USA*
[5]*Columbia University, New York, New York 10027, USA*
[6]*Fermi National Accelerator Laboratory, Batavia, Illinois 60510, USA*
[7]*University of Florida, Gainesville, Florida 32611, USA*
[8]*Indiana University, Bloomington, Indiana 47405, USA*
[9]*Los Alamos National Laboratory, Los Alamos, New Mexico 87545, USA*
[10]*Louisiana State University, Baton Rouge, Louisiana 70803, USA*
[11]*Massachusetts Institute of Technology, Cambridge, Massachusetts 02139, USA*
[12]*Instituto de Ciencias Nucleares, Universidad Nacional Autónoma de México, D.F. 04510, México*
[13]*University of Michigan, Ann Arbor, Michigan 48109, USA*
[14]*Saint Mary's University of Minnesota, Winona, Minnesota 55987, USA*
[15]*Yale University, New Haven, Connecticut 06520, USA*

(Received 8 July 2010; published 26 October 2010)

The MiniBooNE experiment at Fermilab reports results from a search for $\bar{\nu}_\mu \to \bar{\nu}_e$ oscillations, using a data sample corresponding to 5.66×10^{20} protons on target. An excess of 20.9 ± 14.0 events is observed in the energy range $475 < E_\nu^{\mathrm{QE}} < 1250$ MeV, which, when constrained by the observed $\bar{\nu}_\mu$ events, has a probability for consistency with the background-only hypothesis of 0.5%. On the other hand, fitting for $\bar{\nu}_\mu \to \bar{\nu}_e$ oscillations, the best-fit point has a χ^2 probability of 8.7%. The data are consistent with $\bar{\nu}_\mu \to \bar{\nu}_e$ oscillations in the 0.1 to 1.0 eV^2 Δm^2 range and with the evidence for antineutrino oscillations from the Liquid Scintillator Neutrino Detector at Los Alamos National Laboratory.

DOI: 10.1103/PhysRevLett.105.181801 PACS numbers: 14.60.St, 11.30.Er, 14.60.Lm, 14.60.Pq

The MiniBooNE experiment has published searches for $\nu_\mu \to \nu_e$ and $\bar{\nu}_\mu \to \bar{\nu}_e$ oscillations, motivated by the Liquid Scintillator Neutrino Detector (LSND) 3.8σ excess of $\bar{\nu}_e$ candidate events [1]. In the $\nu_\mu \to \nu_e$ study, MiniBooNE found no evidence for an excess of ν_e candidate events above 475 MeV; however, a 3.0σ excess of electronlike events was observed below 475 MeV [2,3]. The source of the excess remains unexplained [3], although several hypotheses have been put forward [4–13], including, for example, anomaly-mediated neutrino-photon coupling, sterile neutrino decay, and sterile neutrino oscillations with *CP* or *CPT* violation. Initial results from the $\bar{\nu}_\mu \to \bar{\nu}_e$ study were reported in [14]. A search in antineutrino mode provides a more direct test of the LSND signal, which was observed with antineutrinos. Because of limited statistics, the initial MiniBooNE $\bar{\nu}_\mu \to \bar{\nu}_e$ search was inconclusive with respect to two-neutrino oscillations at the LSND mass scale, although a joint analysis reported compatibility between the LSND, KARMEN [15,16], and MiniBooNE antineutrino experiments [6]. In this Letter, we report an updated analysis of the $\bar{\nu}_\mu \to \bar{\nu}_e$ search with 1.7 times more protons on target (POT) than reported in [14].

This analysis uses the same technique that was reported earlier [14] and assumes only $\bar{\nu}_\mu \to \bar{\nu}_e$ oscillations with no significant $\bar{\nu}_\mu$ disappearance and no ν_μ oscillations. In addition, no contribution from the observed neutrino-mode low-energy excess has been accounted for in the antineutrino prediction. These simplifications may change the fitted $\bar{\nu}_\mu \to \bar{\nu}_e$ oscillation probability by a total of $\sim$10%.

The antineutrino flux is produced by 8 GeV protons from the Fermilab Booster interacting on a beryllium

 © 2010 The American Physical Society

target inside a magnetic focusing horn. Negatively charged mesons produced in p-Be interactions are focused in the forward direction and subsequently decay primarily into $\bar{\nu}_\mu$. The flux for neutrinos and antineutrinos of all flavors is calculated with a simulation program using external measurements [17]. In antineutrino mode, the ν_μ, $\bar{\nu}_e$, and ν_e flux contaminations at the detector are 15.7%, 0.4%, and 0.2%, respectively. The $\bar{\nu}_\mu$ flux peaks at 400 MeV and has a mean energy of 600 MeV.

The MiniBooNE detector has been described in detail elsewhere [18]. The detector location was chosen to satisfy $L[\mathrm{m}]/E[\mathrm{MeV}] \sim 1$, similar to that of LSND, which maximizes the sensitivity to oscillations at $\Delta m^2 \sim 1$ eV^2. The detector consists of a 40-foot diameter sphere filled with pure mineral oil ($\sim CH_2$). Neutrino interactions in the detector produce final-state electrons or muons, which produce scintillation and Cherenkov light detected by the 1520 8-inch photomultiplier tubes (PMTs) that line the interior of the detector.

The signature of $\bar{\nu}_\mu \to \bar{\nu}_e$ oscillations is an excess of $\bar{\nu}_e$-induced charged-current quasielastic (CCQE) events. Reconstruction [19] and selection requirements of these events are identical to those of the previous neutrino and antineutrino mode analyses [3,14]. The detector cannot distinguish between neutrino and antineutrino interactions on an event-by-event basis. To help constrain the $\bar{\nu}_e/\nu_e$ candidate events, a $\bar{\nu}_\mu/\nu_\mu$ sample is formed. The separation of ν_μ from $\bar{\nu}_\mu$ in this large CCQE sample is accomplished by fitting the observed angular distribution of the outgoing muons to a linear combination of the differing CCQE angular distributions for final state μ^+ and μ^-. Relative to the Monte Carlo prediction, the μ^+ yield required an increase of 1.20 to the rate of π^- decays ($\bar{\nu}_\mu$), while the μ^- yield is 0.99 of its predicted rate. Overall, the normalization required a 13% increase, which is compatible with the combined neutrino flux and cross-section uncertainties [20]. A sample of 24 771 data events pass the $\bar{\nu}_\mu$ CCQE selection requirements. The neutrino and antineutrino content of the sample are 22% and 78%, respectively.

The oscillation parameters are extracted from a combined fit to the $\bar{\nu}_e/\nu_e$ CCQE and $\bar{\nu}_\mu/\nu_\mu$ CCQE event distributions. Any possible $\bar{\nu}_\mu \to \bar{\nu}_e$ signal, as well as some $\bar{\nu}_e$ backgrounds interact through a similar process as $\bar{\nu}_\mu$ CCQE events and are additionally related to the $\bar{\nu}_\mu$ CCQE events through the same π^- decay chain at production. These correlations enter through the off-diagonal elements of the covariance matrix used in the χ^2 calculation, relating the contents of the bins of the $\bar{\nu}_e$ CCQE and $\bar{\nu}_\mu$ CCQE distribution. This procedure maximizes the sensitivity to $\bar{\nu}_\mu \to \bar{\nu}_e$ oscillations when systematic uncertainties are included [21].

The number of predicted $\bar{\nu}_e$ CCQE background events for different ranges of reconstructed neutrino energy (E_ν^{QE}) is shown in Table I. The background estimates include both antineutrino and neutrino events, the latter representing 44% of the total background. The predicted backgrounds to the $\bar{\nu}_e$ CCQE sample are constrained by measurements at MiniBooNE and include neutral current (NC) π^0 events [22], $\Delta \to N\gamma$ radiative decays, and external events from neutrino interactions outside the detector. Other backgrounds from misidentified ν_μ or $\bar{\nu}_\mu$ [23,24] and from intrinsic ν_e and $\bar{\nu}_e$ events from the $\pi \to \mu$ decay chain receive the $\bar{\nu}_\mu$ CCQE normalization correction according to their parentage at production (π^+ or π^-).

TABLE I. The expected (unconstrained) number of events for different E_ν^{QE} ranges from all of the backgrounds in the $\bar{\nu}_e$ appearance analysis and for the LSND expectation (0.26% oscillation probability averaged over neutrino energy) of $\bar{\nu}_\mu \to \bar{\nu}_e$ oscillations, for 5.66×10^{20} POT.

Process	200–475 MeV	475–1250 MeV
ν_μ & $\bar{\nu}_\mu$ CCQE	4.3	2.0
NC π^0	41.6	12.6
NC $\Delta \to N\gamma$	12.4	3.4
External events	6.2	2.6
Other ν_μ & $\bar{\nu}_\mu$	7.1	4.2
ν_e & $\bar{\nu}_e$ from $\mu^\pm$ decay	13.5	31.4
ν_e & $\bar{\nu}_e$ from $K^\pm$ decay	8.2	18.6
ν_e & $\bar{\nu}_e$ from K_L^0 decay	5.1	21.2
Other ν_e & $\bar{\nu}_e$	1.3	2.1
Total background	99.5	98.1
0.26% $\bar{\nu}_\mu \to \bar{\nu}_e$	9.1	29.1

If the low-energy excess observed during neutrino-mode running [2] were scaled by the total neutrino flux, the expected excess for antineutrino mode running would be 12 events for $200 < E_\nu^{\mathrm{QE}} < 475$ MeV. (These events are not included in Tables I and II and in Fig. 1 because they occur below 475 MeV and the origin of these events is unexplained.)

Systematic uncertainties are determined by considering the predicted effects on the $\bar{\nu}_\mu$ and $\bar{\nu}_e$ CCQE rate from variations of actual parameters. These include uncertainties in the neutrino and antineutrino flux estimates, uncertainties in neutrino cross sections, most of which are determined by *in situ* cross-section measurements at

TABLE II. The number of data, fitted (constrained) background, and excess events in the $\bar{\nu}_e$ analysis for different E_ν^{QE} ranges. The uncertainties include both statistical and constrained systematic errors. All known systematic errors are included in the systematic error estimate.

E_ν^{QE} range	Data	Background	Excess
200–475 MeV	119	$100.5 \pm 10.0 \pm 10.2$	18.5 ± 14.3
475–675 MeV	64	$38.3 \pm 6.2 \pm 3.7$	25.7 ± 7.2
475–1250 MeV	120	$99.1 \pm 10.0 \pm 9.8$	20.9 ± 14.0
475–3000 MeV	158	$133.3 \pm 11.5 \pm 13.8$	24.7 ± 18.0
200–3000 MeV	277	$233.8 \pm 15.3 \pm 16.5$	43.2 ± 22.5

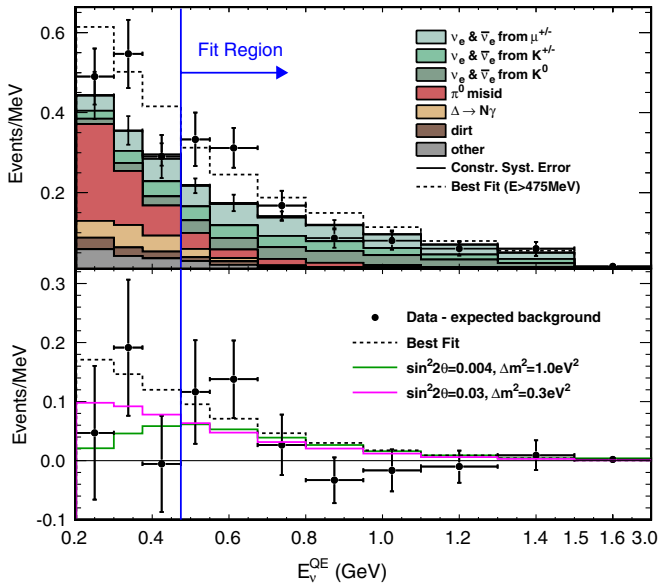

FIG. 1 (color online). Top: The E_ν^{QE} distribution for $\bar{\nu}_e$ CCQE data (points with statistical errors) and background (histogram with systematic errors). Bottom: The event excess as a function of E_ν^{QE}. Also shown are the expectations from the best oscillation fit with $E_\nu^{\mathrm{QE}} > 475$ MeV, $(\Delta m^2, \sin^2 2\theta) = (0.064\ \mathrm{eV}^2, 0.96)$, where the fit is extrapolated below 475 MeV, and from two other oscillation parameter sets in the allowed region. No correction has been made for the low-energy excess of events seen in neutrino mode below 475 MeV. All known systematic errors are included in the systematic error estimate.

MiniBooNE, and uncertainties in detector modeling and reconstruction. By considering the variation from each source of systematic uncertainty on the $\bar{\nu}_e$ CCQE signal, background, and $\bar{\nu}_\mu$ CCQE prediction as a function of E_ν^{QE}, a covariance matrix in bins of E_ν^{QE} is constructed. This matrix includes correlations between $\bar{\nu}_e$ CCQE (signal and background) and $\bar{\nu}_\mu$ CCQE and is used in the χ^2 calculation of the oscillation fit.

Figure 1 (top) shows the E_ν^{QE} distribution for $\bar{\nu}_e$ CCQE observed data and background. A total of 277 events pass the $\bar{\nu}_e$ event selection requirements with $200 < E_\nu^{\mathrm{QE}} < 3000$ MeV, compared to an expectation of $233.8 \pm 15.3 \pm 16.5$ events, where the uncertainty includes both statistical and systematic errors, respectively. This corresponds to an excess of 43.2 ± 22.5 events. (In the previous neutrino run analysis, event totals were considered in two energy regions: 200–475 and 475–3000 MeV, where the latter region was the energy range for the neutrino oscillation search. For the antineutrino data, the excess for $475 < E_\nu^{\mathrm{QE}} < 3000$ MeV is 24.7 ± 18.0 events.) In the energy range from $475 < E_\nu^{\mathrm{QE}} < 1250$ MeV, the observed $\bar{\nu}_e$ events, when constrained by the $\bar{\nu}_\mu$ data events, have a $\chi^2/\mathrm{DF} = 18.5/6$ and a probability of 0.5% for a background-only hypothesis. (This compares to the 40% probability that is observed in neutrino mode [3] for the same energy range.) DF is the effective number of degrees of freedom from frequentist studies. The number of data, fitted background, and excess events for different E_ν^{QE} ranges are summarized in Table II.

Figure 2 shows the observed and predicted event distributions as functions of reconstructed E_{vis} and $\cos(\theta)$ for $200 < E_\nu^{\mathrm{QE}} < 3000$ MeV. E_{vis} is the measured visible energy, while θ is the scattering angle of the reconstructed electron with respect to the incident neutrino direction. The background-only χ^2 values for the $\bar{\nu}_e$ and $\bar{\nu}_\mu$ data are $\chi^2/\mathrm{DF} = 23.8/13$ and $\chi^2/\mathrm{DF} = 13.6/11$ for E_{vis} and $\cos(\theta)$, respectively.

Many checks have been performed on the data to ensure that the backgrounds are estimated correctly. Beam and detector stability checks show that the neutrino event rate is stable to <2% and that the detector energy response is stable to <1%. In addition, the fractions of neutrino and antineutrino events are stable over energy and time, and the inferred external event rates are similar in both neutrino and antineutrino modes. Furthermore, any single background would have to be increased by more than 3σ to explain the observed excess of events. An additional check comes from the data in neutrino mode, which has a similar background to antineutrino mode and where good agreement is obtained between the data and Monte Carlo simulation for $E_\nu^{\mathrm{QE}} > 475$ MeV. As a final check, the event rate of candidate $\bar{\nu}_e$ events in the last 2.27×10^{20} POT is found to be 1.9σ higher than the candidate event rate in the first 3.39×10^{20} POT [14]; however, the $\bar{\nu}_\mu$ event rates are found to be similar for the two running periods.

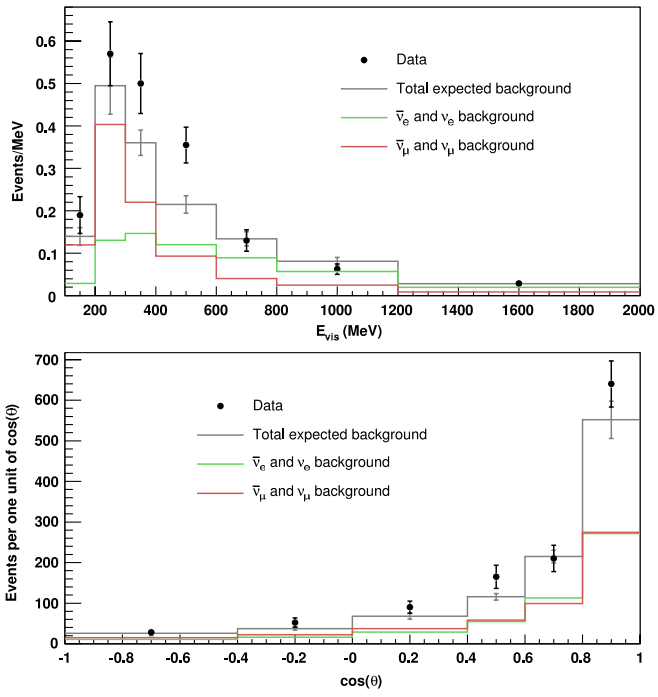

FIG. 2 (color online). The E_{vis} (top panel) and $\cos(\theta)$ (bottom panel) distributions for data (points with statistical errors) and backgrounds (histogram with systematic errors) for $E_\nu^{\mathrm{QE}} >$ 200 MeV.

Figure 1 (bottom) shows the event excess as a function of E_ν^{QE}. Using a likelihood-ratio technique, the best MiniBooNE oscillation fit for $475 < E_\nu^{\mathrm{QE}} < 3000$ MeV occurs at $(\Delta m^2, \sin^2 2\theta) = (0.064\ \mathrm{eV}^2, 0.96)$. The energy range $E_\nu^{\mathrm{QE}} > 475$ MeV has been chosen for the fit as this is the energy range MiniBooNE used for searching for neutrino oscillations. Also, this energy range avoids the region of the unexplained low-energy excess in neutrino mode [3]. This best-fit point has only a slightly lower χ^2 than other points in the allowed band. The χ^2 for the best-fit point in the energy range of $475 < E_\nu^{\mathrm{QE}} < 1250$ MeV is 8.0 for 4 DF, corresponding to a χ^2 probability of 8.7%. The probability of the background-only fit relative to the best oscillation fit is 0.6%. Figure 3 shows the MiniBooNE 68%, 90%, and 99% C.L. closed contours for $\bar{\nu}_\mu \to \bar{\nu}_e$ oscillations in the $475 < E_\nu^{\mathrm{QE}} < 3000$ MeV energy range, where frequentist studies were performed to determine the C.L. regions. The allowed regions are in agreement with the LSND allowed region. The MiniBooNE closed contours for $\bar{\nu}_\mu \to \bar{\nu}_e$ oscillations in the $200 < E_\nu^{\mathrm{QE}} < 3000$ MeV energy range are similar, as shown in Fig. 4. The solid (dashed) curves are without (with) the subtraction of the expected 12 event excess in the $200 < E_\nu^{\mathrm{QE}} < 475$ MeV low-energy region from the neutrino component of the beam. The best oscillation fits without and with this subtraction occur at $(\Delta m^2, \sin^2 2\theta) = (4.42\ \mathrm{eV}^2, 0.0066)$ and $(4.42\ \mathrm{eV}^2, 0.0061)$, respectively, while the corresponding χ^2 probabilities in the $200 < E_\nu^{\mathrm{QE}} < 1250$ MeV energy range are 10.9% and 7.5%.

A further comparison between the MiniBooNE and LSND antineutrino data sets is given in Fig. 5, which shows the oscillation probability as a function of L/E_ν for $\bar{\nu}_\mu \to \bar{\nu}_e$ candidate events in the L/E_ν range where MiniBooNE and LSND overlap. The data used for LSND and MiniBooNE correspond to $20 < E_\nu < 60$ MeV and $200 < E_\nu^{\mathrm{QE}} < 3000$ MeV, respectively. The oscillation probability is defined as the event excess divided by the number of events expected for 100% $\bar{\nu}_\mu \to \bar{\nu}_e$ transmutation, while L is the reconstructed distance traveled by the antineutrino from the mean neutrino production point to the interaction vertex and E_ν is the reconstructed antineutrino energy. The L/E_ν distributions for the two data sets are consistent.

In summary, the MiniBooNE experiment observes an excess of $\bar{\nu}_e$ events in the energy region above E_ν^{QE} of 475 MeV for a data sample corresponding to 5.66×10^{20} POT. A model-independent hypothesis test gives a probability of 0.5% for the data to be consistent with the expected backgrounds in the energy range of $475 < E_\nu^{\mathrm{QE}} < 1250$ MeV, and a likelihood-ratio fit gives a 0.6% probability for background-only relative to the best oscillation fit. The allowed regions from the fit, shown in Fig. 3, are consistent with $\bar{\nu}_\mu \to \bar{\nu}_e$ oscillations in the 0.1 to 1 eV^2

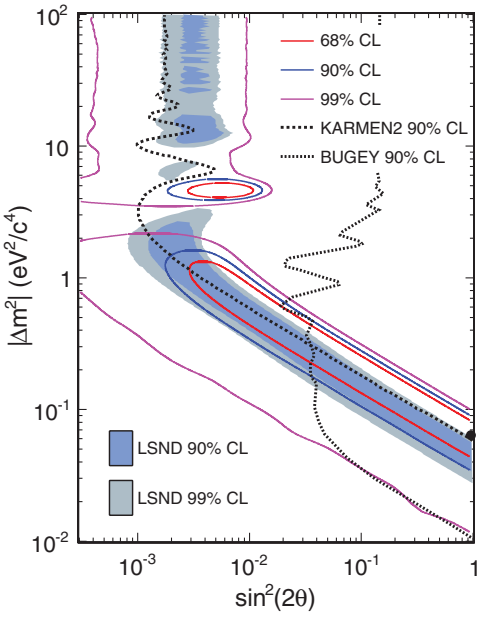

FIG. 3 (color online). MiniBooNE 68%, 90%, and 99% C.L. allowed regions for events with $E_\nu^{\mathrm{QE}} > 475$ MeV within a two-neutrino $\bar{\nu}_\mu \to \bar{\nu}_e$ oscillation model. Also shown are limits from KARMEN [15] and Bugey [25]. The Bugey curve is a 1-sided limit for $\sin^2 2\theta$ corresponding to $\Delta\chi^2 = 1.64$, while the KARMEN curve is a "unified approach" 2D contour. The shaded areas show the 90% and 99% C.L. LSND allowed regions. The black dot shows the best-fit point.

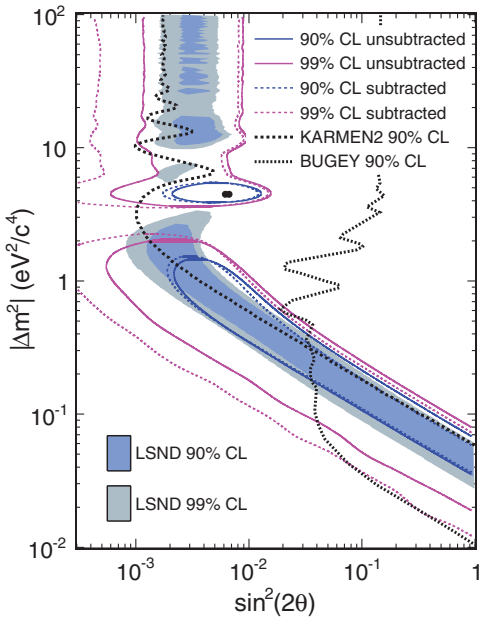

FIG. 4 (color online). MiniBooNE 90% and 99% C.L. allowed regions for events with $E_\nu^{\mathrm{QE}} > 200$ MeV within a two-neutrino $\bar{\nu}_\mu \to \bar{\nu}_e$ oscillation model. The solid (dashed) curves are without (with) the subtraction of the expected 12 event excess in the $200 < E_\nu^{\mathrm{QE}} < 475$ MeV low-energy region from the neutrino component of the beam. Also shown are limits from KARMEN [15] and Bugey [25]. The shaded areas show the 90% and 99% C.L. LSND allowed regions. The black dots show the best-fit points.

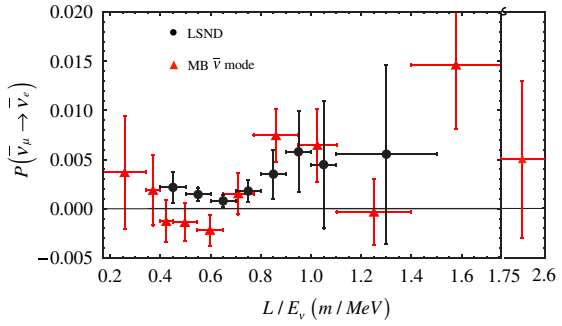

FIG. 5 (color online). The oscillation probability as a function of L/E_ν^{QE} for $\bar{\nu}_\mu \to \bar{\nu}_e$ candidate events from MiniBooNE and LSND. The data points include both statistical and systematic errors.

Δm^2 range and consistent with the allowed region reported by the LSND experiment [1]. Additional running in anti-neutrino mode is expected to approximately double the current number of POT.

We acknowledge the support of Fermilab, the Department of Energy, and the National Science Foundation, and we acknowledge Los Alamos National Laboratory for LDRD funding. We also acknowledge the use of CONDOR software for the analysis of the data.

*Present address: IFIC, Universidad de Valencia and CSIC, Valencia 46071, Spain.

†Present address: Imperial College, London SW7 2AZ, U.K.

[1] C. Athanassopoulos *et al.*, Phys. Rev. Lett. **75**, 2650 (1995); **77**, 3082 (1996); **81**, 1774 (1998); Phys. Rev. C **58**, 2489 (1998); A. Aguilar *et al.*, Phys. Rev. D **64**, 112007 (2001).

[2] A. Aguilar-Arevalo *et al.*, Phys. Rev. Lett. **98**, 231801 (2007).

[3] A. A. Aguilar-Arevalo *et al.*, Phys. Rev. Lett. **102**, 101802 (2009).

[4] J. A. Harvey, C. T. Hill, and R. J. Hill, Phys. Rev. Lett. **99**, 261601 (2007); Phys. Rev. D **77**, 085017 (2008).

[5] S. N. Gninenko, Phys. Rev. Lett. **103**, 241802 (2009); S. N. Gninenko and D. S. Gorbunov, Phys. Rev. D **81**, 075013 (2010).

[6] G. Karagiorgi *et al.*, Phys. Rev. D **80**, 073001 (2009).

[7] M. Sorel, J. M. Conrad, and M. H. Shaevitz, Phys. Rev. D **70**, 073004 (2004); G. Karagiorgi *et al.*, Phys. Rev. D **75**, 013011 (2007); A. Melchiorri *et al.*, J. Cosmol. Astropart. Phys. 01 (2009) 036; M. Maltoni and T. Schwetz, Phys. Rev. D **76**, 093005 (2007).

[8] H. Pas, S. Pakvasa, and T. J. Weiler, Phys. Rev. D **72**, 095017 (2005).

[9] T. Goldman, G. J. Stephenson, and B. H. J. McKellar, Phys. Rev. D **75**, 091301 (2007).

[10] V. Barger, D. Marfatia, and K. Whisnant, Phys. Lett. B **576**, 303 (2003).

[11] E. Akhmedov and T. Schwetz, arXiv:1007.4171.

[12] A. E. Nelson and J. Walsh, Phys. Rev. D **77**, 033001 (2008).

[13] V. A. Kostelecky and M. Mewes, Phys. Rev. D **69**, 016005 (2004); T. Katori, V. A. Kostelecký, and R. Tayloe, Phys. Rev. D **74**, 105009 (2006).

[14] A. Aguilar-Arevalo *et al.*, Phys. Rev. Lett. **103**, 111801 (2009).

[15] B. Armbruster *et al.*, Phys. Rev. D **65**, 112001 (2002).

[16] E. D. Church *et al.*, Phys. Rev. D **66**, 013001 (2002).

[17] A. A. Aguilar-Arevalo *et al.*, Phys. Rev. D **79**, 072002 (2009).

[18] A. A. Aguilar-Arevalo *et al.*, Nucl. Instrum. Methods Phys. Res., Sect. A **599**, 28 (2009).

[19] R. B. Patterson *et al.*, Nucl. Instrum. Methods Phys. Res., Sect. A **608**, 206 (2009).

[20] A. A. Aguilar-Arevalo *et al.*, Addendum to the MiniBooNE Run Plan: MiniBooNE Physics in 2006 (Fermilab, Batavia, IL, 2006).

[21] D. W. Schmitz, Report No. FERMILAB-THESIS-2008-26.

[22] A. A. Aguilar-Arevalo *et al.*, Phys. Lett. B **664**, 41 (2008); Phys. Rev. D **81**, 013005 (2010).

[23] A. A. Aguilar-Arevalo *et al.*, Phys. Rev. Lett. **100**, 032301 (2008).

[24] A. A. Aguilar-Arevalo *et al.*, Phys. Rev. Lett. **103**, 081801 (2009).

[25] B. Achkar *et al.*, Nucl. Phys. B **434**, 503 (1995).